Optimization of Operating Profit for the FEED of the PZAS™ process for CO_2 Capture on a 460 MW NGCC

Athreya Suresh Babu[a], Miguel Abreu[a], Benjamin Drewry[a], Yee Lee Chen[a], Gary T. Rochelle[a,]*

[a] Texas Carbon Management Program, McKetta Department of Chemical Engineering, The University of Texas at Austin, 10500 Exploration Way, Austin, TX 78758, USA

email: gtr@che.utexas.edu[*]

ABSTRACT A rating model of PZAS (Piperazine with the Advanced Stripper) for a 460 MW natural gas combined cycle was developed from vendor-provided equipment performance data. Surrogate rating models were built and used to optimize variable profit of the system subject to natural gas and electricity price at a fixed value for CO_2 of $80/tonne. Several process constraints were considered between ambient temperatures of 4.4 and 40.5 °C. Lower lean loading resulted in lower reboiler heat duty of about 2.2 GJ/tonne. Lean loading at 0.2 mol/equiv N was sufficient at an ambient temperature of 4.4 ˚C to maximize variable profit. Solvent precipitation was avoided

even at low lean loading (0.18 mol/mol) in the absence of a trim cooler for the lean solvent between the absorber and the cold cross exchanger. Optimal CO_2 removal was always higher than the design case removal of 90% and achieved a peak of 93.6% for 4.4 °C ambient temperature. Lean solvent rate was a significant driver of profitability. The maximum capacity of the compressor was a significant constraint on profitability. Increasing compressor capacity by 20–30% could increase variable profit by about 21% in the case of 0.18 lean loading at 4.4 ˚C ambient temperature. This increase in profit was lower at higher ambient temperature and higher lean loading.

The breakeven gas price was $4.6/MMBtu at high lean loading of 0.22 mol/mol. Below this value, profit was maximized by increasing the boiler heat rate. Above this value, profit could not be increased by burning additional natural gas, requiring a reduction in boiler heat rate and consequently, specific heat duty. At lower lean loading (0.2, 0.18 mol/mol), this transition in heat duty was not observed due to the lower heat duty. As the ambient temperature increased, a similar trend in heat duty was observed at 0.22 lean loading, but the transition to lower heat duty occurred earlier at $4/MMBtu. This was because of the lower CO_2 production at higher ambient temperature, making the process unprofitable at a gas price higher than $3/MMBtu unless the heat duty of the stripper and natural gas boiler is steeply decreased.

Introduction

The Texas Carbon Management Program developed a Front-End Engineering Design (FEED) of the Piperazine Advanced Stripper (PZAS) process at an existing 460 MW NGCC in West Texas. The details of the design of the absorber, stripper, and other equipment are provided by Gao [1], Suresh Babu [2], and Closmann et al. [3]. Additional details on the FEED are reported by Rochelle et al. [4, 5]. With a finalized design for the facility in Aspen Plus® [6], rating models for the absorber, stripper, air coolers, water wash, and compressors were developed by incorporating real equipment performance data obtained from vendors. The rating models were then used to identify equipment that limited the performance of the facility. The general modeling methods are described in the 'modeling methods' sections and the specifics of the rating models are described in the 'rating model specifications' sections. For ease of convergence, faster simulation times, and equation-oriented modeling and optimization, surrogate models of all the rating models were built using the ALAMO Model Building Tool [7], which resulted in accurate algebraic equations for heat and mass flows within the system. More details on the construction of the surrogate models are provided in the 'surrogate model development' sections and the models themselves are presented in Appendix E in the supplementary material. These equations were simultaneously

solved using MATLAB [8] with 7 major independent variables that determined system performance. These were the lean solvent rate, number of air cooler bays, cold rich bypass flowrate, warm rich bypass flowrate, number of water wash pumps, number of intercooler pumps, and lean loading at constant stripping temperature of 150 ℃. Lean loading has an uncertain constraint associated with the precipitation of piperazine hexahydrate when the system must shut down. During normal operation the process can be constrained by monitoring the loading and temperature of the cold lean solvent. However, precipitation may occur if the system shuts down and lean solvent cools to a much lower temperature. Therefore, arbitrarily low lean loading values of 0.2 and 0.18 have been considered for this work.

These independent variables were optimized to maximize the variable profit, which considered the cash flow related to gas and power consumption, and revenue from CO_2. These factors depended on gas price, power price, the market value of CO_2, and ambient temperature. The dependent variables such as rich loading, CO_2 removal, and heat duty were optimized by maximizing the variable profit using the independent variables. This analysis was done with variable flue gas specifications corresponding to ambient temperature of 4.44, 18.33, and 40.5 ˚C. These results define optimal tuning of the plant operation to always maximize the variable profit.

More details on this are given in Appendix C (in the supplementary material) as well as in the 'optimization of variable profit in MATLAB', 'results and discussion,' and 'conclusions' sections; the MATLAB subroutine itself is given in Appendices E and F (in the supplementary material).

Nomenclature

$\$_{CO2}$	value of CO_2, \$/tonneCO_2
$\$_{Elect}$	electricity cost, \$/MWh
$\$_{NG}$	cost of natural gas, \$/MMBtu
$N_{TrainsX}$	number of process trains online
$Power_X$	total power requirement of capture plant, MW
Profit	variable profit rate for capture system, \$/hr
$Rate_{CO2}$	flowrate of CO_2 produced by capture system, tonne/hr
$Rate_{NG}$	rate of natural gas consumed by gas-fired boiler, MMBtu/hr

Modeling Methods

The rating models developed in this work were created in the Aspen Plus® software. The Independence™ model was used to estimate solvent thermodynamics, reaction kinetics, and the physical properties of the 5 m PZ solvent [9]. The performance of the structured packing in the absorber and random packing in the stripper was estimated using the model developed by Song at the University of Texas Separations Research Program (UT-SRP) [10]. This model can estimate k_L, k_G, and wetted area for structured, hybrid, and random packings and includes the effect of liquid viscosity on k_L. This section provides an overview of the different parts of the rating model and how they relate to the PZAS FEED base case. The PZAS process flowsheet is shown in Figure 1.

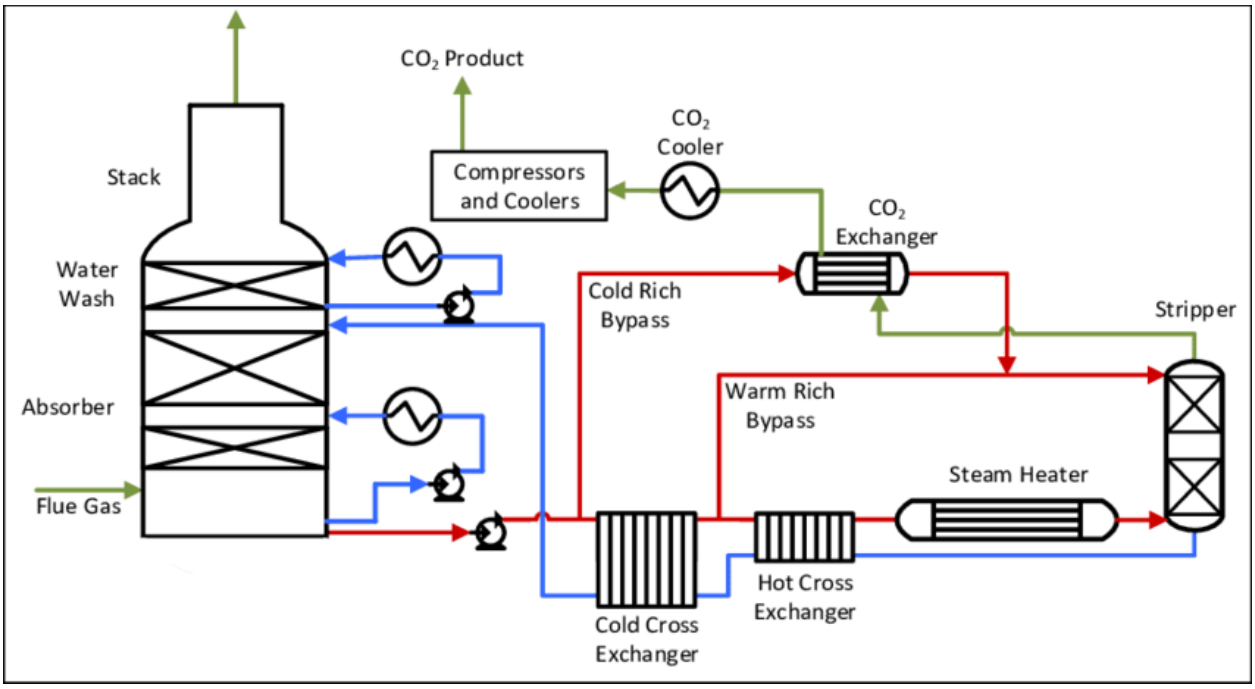

Figure 1: PZAS process flowsheet

Absorber

The Mustang FEED absorber was designed for a baseline CO_2 removal rate of 90%. The system is composed of two absorber trains, each with a square cross section with an area of 174 m^2. MellapakPlus™ 252Y (M252Y) structured packing was used in all sections to minimize the pressure drop across the column. The height of the packing sections was 4.9 and 2.7 m, from top to bottom. Flue gas from the natural gas boiler used to supply regeneration steam was mixed with flue gas from the Heat Recovery Steam Generator (HRSG) and fed to the bottom of the absorber. The boiler flue gas flow was about 10% of the HRSG flue gas flow at design conditions.

The absorber model included the absorber unit, the fans upstream of the absorber, a pressure drop model, and the natural gas-fired boiler model. A RadFrac block in Aspen Plus® was used to model the rate-based mass transfer in the absorber. A diameter of 14.9 m was used, which gave the same cross-sectional area as the rectangular Mustang FEED absorber. The HRSG flue gas flowrate, temperature, and composition were different for each ambient temperature case studied. The specifications for the 18.33 and 40.5 ˚C cases were obtained directly from the mass balance provided by GSEC (Golden Spread Electric Cooperative), whereas the specifications for the 4.44 ˚C case were obtained by interpolation. Table 1 shows the HRSG gas specifications for all cases studied.

Table 1: HRSG flue gas specifications for all cases studied in this work

Case	A	B	C	D	E
(Amb. T, HRSG Flue Gas %, Duct Burn.)	4.44 ˚C, 95%, No DB	18.33 ˚C, 72%, No DB	18.33 ˚C, 95%, No DB	18.33 ˚C, 100%, DB	40.5 ˚C, 95%, No DB
Temperature (˚C)	105.6	104.5	104.5	104.5	103

Flowrate (lb/hr)	3,432,795	2,283,803	3,010,027	3,172,189	2,841,211
CO_2 (mol %)	3.84	3.84	3.84	3.99	3.82
H_2O (mol %)	7.93	8.53	8.53	8.81	10.08
N_2 (mol %)	75.54	75.05	75.05	74.24	73.80
O_2 (mol %)	12.69	12.58	12.58	12.95	12.30

The vendor-provided gas-fired boiler specification sheets were used to regress the flue gas flowrate, temperature, and composition as a function of plant load. These correlations were used to define the conditions of the boiler flue gas fed to the absorber. The HRSG and boiler flue gas fans were modeled using the fan models in Aspen Plus® and the information from vendor quotes.

Water Wash

The water wash was located above the solvent contacting section of the absorber and was composed of a single bed of M252Y packing. The height of the packing section was 3.048 m. A RadFrac block was used in Aspen Plus® to model the performance of the water wash. The liquid and gas-film mass transfer coefficients were estimated using the model developed by Song [10].

The heat transfer coefficient was estimated from the binary mass transfer coefficients using the Chilton and Colburn method [11].

Air Coolers

The air coolers for the water wash and pump-around cooling loops were modeled in the Aspen Plus® Exchanger Design and Rating (EDR) software [12]. The cooling air was specified in accordance with the site-specific pressure gauge (psig) data. The air cooler geometries and fan curves from vendor quotes were supplied to EDR to specify the type and performance of the FEED air coolers. The model was reduced to a single air cooler bay from the vendor quote and then scaled up to the desired flowrate and number of bays in operation. The feasibility of the liquid-side flowrates was determined by the pump capacity and pressure drop requirements.

Stripper

The stripper column was modeled using rate-based modeling in Aspen Plus® using the RadFrac option. A constant 0.16 correction factor was applied to the wetted mass transfer area [13] in the stripper column to bridge discrepancies between measured and modeled diffusivity of PZ in the column. The heat exchangers were modeled using pairs of heater blocks for ease of convergence. The NTU (number of heat transfer units) of the heat exchanger using the lean solvent temperature difference was specified to define their areas. The NTU of the cold and hot cross exchangers were

defined using the lean-side temperature difference and the Log-Mean Temperature Difference (LMTD) of the cross exchangers as shown by Equation 1. This method of defining heat exchanger performance yields the same set of temperatures on both sides of the cross exchanger irrespective of scale or flowrate.

$$NTU = \frac{\Delta T_{lean}}{LMTD} \quad (1)$$

The design used 2 stripper trains, each of which had three cold cross exchangers, two hot cross exchangers, a stripper column, a CO_2 exchanger, and a condenser. Each stripper column had a total height of 7.5 m and consisted of two sections of random packing: 3.75 m of RSR 2 packing at the top and 3.75 m of RSR 3 packing at the bottom. The cold cross exchanger was designed with a NTU of 5.3, the hot cross exchanger with a NTU of 1.7, and the CO_2 exchanger with a NTU of 3.88.

Rating Model Development

The rating model was built in Aspen Plus® to represent semi-dynamic process performance. This involved modeling equipment that would typically not be included in a design model, such as the performance of pumps and fans, the pressure drop in the system, and typical operational constraints. Some of the equipment in the process was modeled by either coding an algebraic

model into the Aspen Plus® software using calculator blocks or by using other Aspen Plus® tools such as the EDR software [12]. The required changes to the design model are described in detail in Appendix A in the supplementary material.

Surrogate Model Development

The Aspen Plus® rating models were used to collect data over an operational range of interest for the different cases listed in Table 1. These data were used with the ALAMO software to generate surrogate models for each section of the PZAS process. These were essentially algebraic models which represent various independent variables in the process. This allowed for much faster computation compared to Aspen Plus® while still retaining its accuracy and the semi-dynamic characteristics of the rating models. Appendix B in the supplementary material summarizes all the surrogate models developed and the ranges for which they are applicable. The mathematical form of all surrogate models can be found in Appendix E in the supplementary material.

Integrated Process Surrogate Model for PZAS using MATLAB

The MATLAB software was used to study the off-design performance of the PZAS process. A script was written for this purpose which contains all the surrogate models and an algorithm to converge all models for a given set of independent variables. An additional script was developed

to determine the optimum profit rate for each of the cases studied. Appendix C in the supplementary material details the workings of all MATLAB scripts, which are provided in Appendices E and F, also in the supplementary material. The PZAS process script has several feasibility flags that represent process constraints. These are shown in Table 2.

Table 2: PZAS process surrogate model feasibility flags

Feasibility Flags	Constraint
Cold and Warm Rich Bypass Flowrates	CO_2 exchanger cold side pinch
Lean Pump Operation	Pump cavitation
Rich Pump Operation	Max. head
CO_2 Compressor Operation	Max. Capacity
Gas-fired Boiler	Max. Capacity
Gas-fired Boiler Fan	Max. Capacity
Stripper Flooding	100% Flooding
Absorber Flooding	100% Flooding
Solvent Precipitation	Minimum temperature

Figure 2 shows a flowchart summarizing the MATLAB script simulation process to obtain steady-state results with the PZAS process model. A complete description of the diagram can be found in Appendix C in the supplementary material.

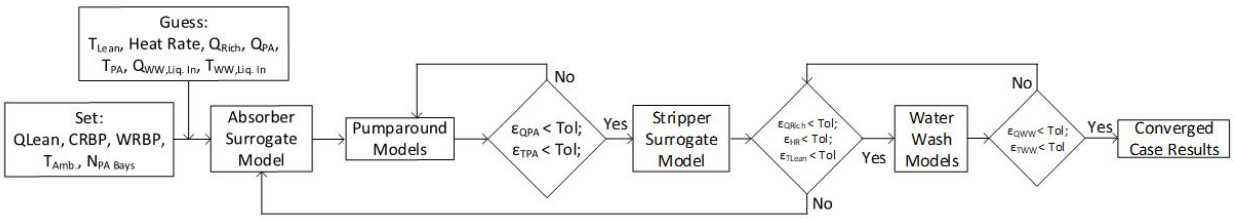

Figure 2: Steady-state convergence scheme used in PZAS™ process MATLAB script

Optimization of Variable Profit in MATLAB

Operating conditions of the plant were optimized to maximize the variable profit rate shown in Equation 2.

$$Profit = N_{Trains}(\$_{CO_2}Rate_{CO_2} - \$_{Elect.}Power - \$_{NG}Rate_{NG}) \quad (2)$$

Various conditions were studied such as changes in gas and power price, ambient temperature swings, and the amount of HRSG flue gas processed by the absorbers to reflect the different cases in Table 1. The use of duct burning of natural gas to increase the power production was considered in case D. Two gas prices, \$3 and \$5/MMBtu were considered for this analysis. The price of electricity was calculated using a nominal heat rate of 7000 Btu heat/kWh electricity to which a surcharge of \$5/MWh was added. Details on the optimization method and equations are provided

in Appendices B to F in the supplementary material. Ultimately, this resulted in 10 cases (5 cases with 2 gas and power prices each), summarized in Table 3.

Table 3: Specifications for cases studied in this work

HRSG flue gas (%)	Ambient T (˚C)	Gas price ($/MMBtu)	Power price ($/MWh)
95% with no duct burning	4.4	3	26
		5	40
100% + duct burning	18.3	3	26
		5	40
72% with no duct burning	18.3	3	26
		5	40

95% with		3	26
no duct	18.3		
		5	40
burning			
95% with		3	26
no duct	40.5		
		5	40
burning			

Table 4 summarizes the results of this analysis at a gas price of $3/MMBtu.

Table 4: Results from the PZAS variable profit optimization for gas price of $3/MMBtu; all numbers except profit are for one process train; CO_2 value: $80/tonne

Case	A	B	C	D	E	Design Case
	4.4, 95,	18.3, 72,	18.3, 95,	18.3, 100	40.5, 95,	

(T_{AMB} ˚C, HRSG Flue Gas %, Duct Burning)	No DB	No DB	No DB	DB	No DB	18.33, 100, DB
Hourly Profit ($/hr)	14,116	10,594	12,938	13,724	11,637	12,968
CO_2 Production (t/hr)	102	76	93	99	84	94.8
CO_2 Removal (%)	93.6	98	96	94	93	90
Lean Ldg (mol/mol)	0.207	0.180	0.193	0.207	0.184	0.2
Rich Ldg (mol/mol)	0.381	0.365	0.368	0.377	0.352	0.4
Lean solvent rate (kg/s)	549	386	503	546	475	450

Air cooler bays for intercooling	18	18	20	17	20	20
Intercooler solvent T, out (℃)	23	30.5	31	31.8	45.6	29.4
Rich solvent T (℃)	43	44	46	47	53	44
Air cooler bays for water wash	6	5	8	10	18	18
Electric power (MW)	31	21	28	30	28	34
Heat Duty (MMBTU/hr)	233	169	209	221	186	272

Specific heat duty (GJ/t)	2.26	2.208	2.22	2.21	2.19	3.0
Cold lean solvent T (°C)	71	71	73	74	78	61
Boiler capacity (% max)	70.9	51.4	63.5	67.1	56.5	98.2
Compressor capacity (% max)	100	89	99	100	100	96
Boiler fan speed (% max)	91.7	63.3	81	85.7	76	99.7

Results and Discussion

Air Cooler Operation for Intercooling

For 4.4 ˚C ambient temperature 18 air cooler bays and both pumps were used for absorber intercooling. At ambient temperature of 18.3 ˚C and 40.5 ˚C, the number of intercooler bays increased to 20 with both pumps in use. This was expected since the number of bays used is directly

proportional to the absorber performance, and higher ambient temperatures required more cooling to maximize the rich loading at the bottom of the absorber. The temperature of the rich solvent leaving the intercooler was 23, 31, and 45.6 ℃ at 4.4, 18.3, and 40.5 ˚C ambient temperature respectively, with 95% HRSG flue gas. The increase in rich solvent temperature reflects the increase in the temperature of the ambient air used in the air cooler bays.

In general, the number of intercooler bays was close to maximum for each case because the flue gas inlet to the absorber was at an elevated temperature of 112 ˚C or higher. Because no direct contact cooler (DCC) was used, the pump-around section was used to cool the flue gas and consequently the absorber column. The temperature management issue in the absorber was compounded by the lack of a trim cooler in the design, which made for high lean solvent temperature, ranging from 71 to 78 ℃. However, the presence of a trim cooler would likely not produce a drastically different profit optimum, unless cooling water were to be used, which would likely increase the profit for all cases. Cooling water would probably produce more uniform optimum conditions between cases since the system would be less exposed to differences in ambient temperature.

Air Cooler Operation for Water Wash

Water wash operation was determined by selecting the number of air cooler bays, out of a total of 18, that minimized the difference between the amount of water in the flue gas inlet and in the water wash gas outlet. A higher number of bays correspond to a higher liquid flowrate in the water wash. For the 4.44 and 18.33 ˚C cases, 6 and 8 bays and one water wash pump were required to minimize the difference in water vapor, respectively. The number of required bays increased with HRSG flue gas flowrate and decreased with ambient temperature. At 18.3 ˚C, with 100% of the HRSG flue gas, the optimization resulted in 10 air cooler bays being used. This number decreased to 8 with 95% of the HRSG flue gas and to 5 with 72% of the HRSG flue gas at the same ambient temperature. For the 40.5 ˚C case, optimal operation required all 18 air cooler bays and one water wash pump. This increase in number of bays compared to the other cases was expected since the higher ambient temperature makes for a hotter inlet liquid stream in the water wash and hotter CO_2-lean flue gas into the water wash.

Absorber Flooding

Flooding in the bottom section of the absorber was never higher than 84% for any of the cases studied. The higher values observed for this variable pertained to the 4.44 ˚C with 95% HRSG flue

gas and 18.3 ˚C with 100% HRSG flue gas cases, which correspond to the two highest flue gas flowrates of all cases studied.

Stripper Flooding

The highest observed stripper flooding was 97% in the bottom section of the column for the 4.4 ˚C case with 95% HRSG flue gas. The 18.3 and 40.5 ˚C cases had lower flooding at 88% and 84% respectively in the bottom section of packing. This could be explained by a monotonic decrease in lean solvent rate and CO_2 flowrate with an increase in ambient temperature. Both the liquid and vapor rate in the stripper determined the flooding in the column. This flooding was usually the greatest at the bottom of the lower packing section where the liquid and vapor rate is usually the highest. At this point, the liquid has picked up the most water through direct condensation in the column and the vapor has the highest velocity due to the lowest pressure drop experienced.

Approach to Maximum Boiler Heat Rate

The boiler heat rate did not exceed the maximum boiler capacity in any of the cases. The approach to maximum boiler heat rate (%) ranged from 56.5–70.9%. The approach to maximum boiler capacity was correlated well with the percentage of HRSG flue gas processed by the system at constant temperature. With increasing ambient temperature at 95% HRSG flue gas, the approach

to maximum boiler capacity decreased monotonically, which is related to the consistent decrease in boiler heat rate (and flue gas produced) with increasing ambient temperature. Although the rich loading decreased with increasing temperature, the gross heat rate of the boiler is only related to the amount of CO_2 processed by the system, which decreased consistently with ambient temperature. Higher ambient temperature cases also had a lower mass flowrate of flue gas due to a lower gas density.

Approach to Maximum Compressor Capacity

For 95% HRSG flue gas, the approach to maximum compressor capacity (%) ranged from 99-100% between 4.4 and 40.5 ˚C. The compressor was at its maximum capacity for both the low temperature (4.4 ˚C) and high temperature (40.5 ˚C) cases. This was expected because CO_2 flowrate is an important driver of variable profit of the plant, which is to be maximized at any given condition in this work. At a fixed ambient temperature of 18.3 ˚C, with an increasing percentage of HRSG flue gas, the approach to maximum compressor capacity (%) increased owing to the larger amount of CO_2 in the flue gas.

Approach to Maximum Gas-fired Boiler Fan Speed

The boiler fan speed also did not exceed the maximum in any of the cases. Approach to maximum boiler fan speed (%) ranged from 76–91.7% and was correlated to the percentage of HRSG flue gas processed by the system at constant temperature. With increasing ambient temperature at 95% HSRG flue gas, the approach to maximum boiler fan speed decreased, because of the concurrent decrease in boiler heat rate. The boiler and boiler fans appear to be overdesigned.

Effect of Process Constraints on Maximum Achievable Variable Profit with Varying Ambient Temperature

The optimization model used 9 constraints in total. This section analyzes the change in optimum variable profit (%) when the number of constraints applied to the optimization is decreased.

In the figure below, going from right to left, each constraint in the optimization is removed. For example, first, the precipitation constraint is removed. Next, the compressor capacity constraint is removed on top of the precipitation constraint, and so on. The case on the far right in Figure 3 represents the lowest attainable profit with all 9 process constraints. The optimum profit achieved for the cases to its left was compared to this value to calculate a change in maximum profit (%).

This analysis has been done for a gas price of $3/MMBtu, for three different lean loadings at 4.4, 18.3, and 40.5 ˚C ambient temperature with 95% HRSG flue gas.

The precipitation constraint was not violated under any condition, so removing it did not change the profit regardless of lean loading or ambient temperature.

For 4.4 ℃ ambient temperature:

Removing the compressor capacity constraint sizably increased the attainable maximum profit by about 20.9% for 0.18 lean loading. At low lean loading, a higher CO_2 flowrate is processed owing to the high rich loading, and the compressor capacity constrains the system. The compressor capacity is exceeded by 20–30% with varying lean loading. The absorber and stripper flooding did not limit the variable profit. Removing the boiler fan constraint required that the boiler fan capacity and compressor capacity be increased by 8 and 24% respectively to increase profit by 21.1%. Removing the boiler capacity constraint required that the boiler, boiler fan, and compressor be increased by 33, 34, and 30%, respectively, to increase the profit by 21.45%. The pumps and bypass constraints did not affect profit.

At 0.2 lean loading, only the compressor limited the process. A 2% increase in compressor capacity can increase the variable profit by 1.7%.

At 0.22 lean loading, only the stripper flooding limited the profit. A 3% increase in stripper capacity can change the variable profit by 0.52%. This was due to the highest solvent rate at high lean loading.

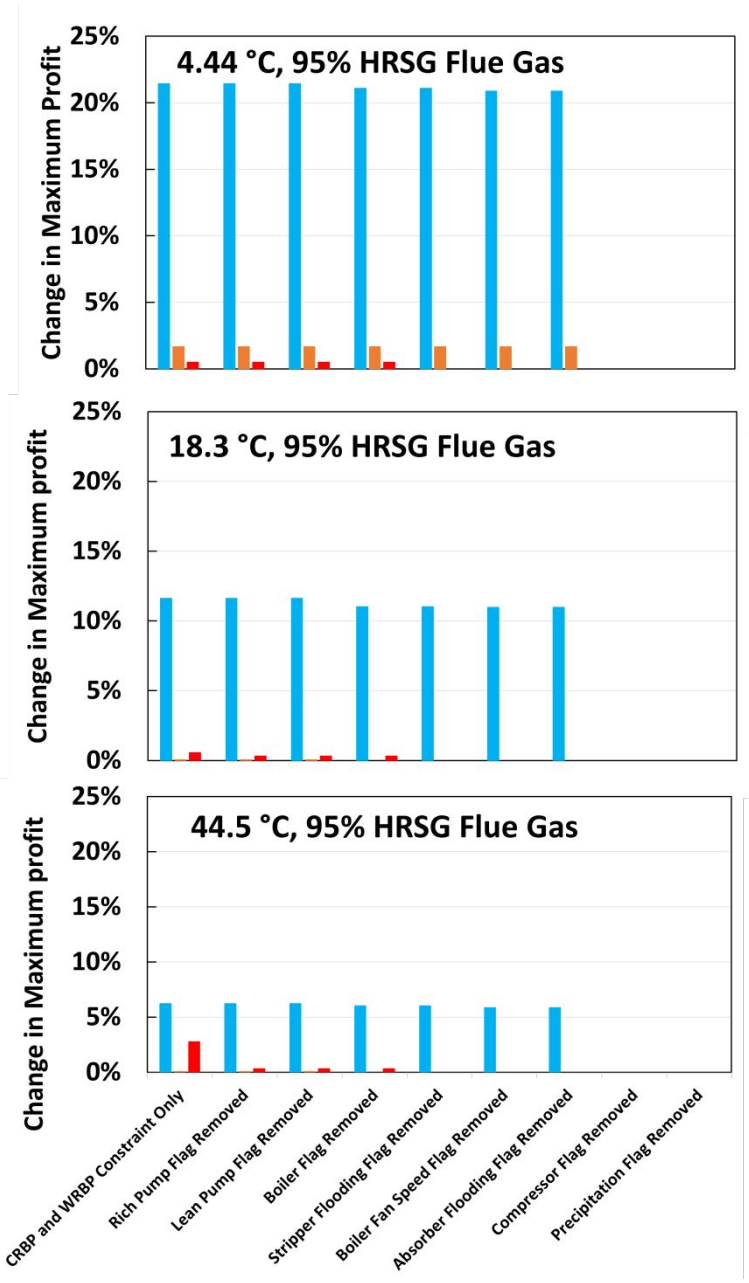

Figure 3. Effect of removing different process constraints on profitability at different ambient temperatures with 95% HRSG flue gas; gas price = $3/MMBtu

At 18.3 ℃ ambient temperature:

At 0.2 lean loading, like the low temperature case, the compressor, boiler fan, and boiler were the only limiting equipment. Profitability was impacted by a smaller degree due to the lower CO_2 flowrate already processed by the system. Increasing compressor capacity by 15% can result in a 11% increase in profit. A 2% increase in boiler fan capacity had to be accompanied by a 16% increase in compressor capacity to increase profit (+11.03%). A 30% increase in boiler capacity had to be accompanied by a 26 and 21% increase in boiler fan and compressor capacity, respectively, to increase profit (+11.62%).

At 0.2 lean loading, removing the boiler capacity constraint required a 4% increase in boiler fan capacity to yield marginal increase in profit (+0.06%).

At 0.22 lean loading, increasing stripper and rich pump capacity minimally impacted profit (+0.32-0.56%).

At 44.5 ℃ ambient temperature:

At 0.18 lean loading, an 11% increase in compressor capacity only resulted in 5.9% increase in profit. Boiler fan capacity can be increased by 16% and boiler capacity can be increased by 2-16% to increase profit (+6.05-6.24%) if the compressor capacity was also increased by 12-15%. Other equipment did not limit the profit.

At 0.2 lean loading, increasing the capacity of the boiler required a 3% increase in boiler fan capacity to obtain marginal improvement (+0.1%) in profit.

At 0.22 lean loading, increasing the rich pump capacity impacted profit (+2.78%) more than increasing the stripper capacity (+0.33%).

Optimal Operation Over a Wide Range of Gas Prices

Figure 4 shows the dependence of optimum specific heat duty on a wide range of gas prices at three different lean loading and ambient temperature/flue gas cases. The figure indicates that a lower lean loading will always provide a lower energy requirement for regeneration, irrespective of gas price and ambient temperature. This also demonstrates that PZAS can operate flexibly with an energy requirement of 2.2–3 GJ/tonne at variable ambient temperature and lean loading. A similar decrease in regeneration energy requirement with decreasing lean loading was observed in

the pilot test of the PZAS at the UT-SRP pilot plant and was documented by Suresh Babu and Rochelle [14].

Figure 4 also demonstrates an independent effect of gas price on heat duty. At 0.22 lean loading and gas price between $3 and 4/MMBtu, heat duty was the highest compared to other lean loadings. As the gas price increased to $5/MMBtu, the heat duty dropped to about 2.3 GJ/tonne and from there on monotonically decreases with increasing gas price. This can be explained by calculating a "breakeven" gas price that produces a value for the emitted CO_2 exactly equal to $80/tonne.

Assuming natural gas was methane only, the LHV (low heating value) of 21,496 Btu/lb was used for this calculation. Assuming the complete combustion of methane, the breakeven gas price was $4.6/MMBtu. Below this value, the variable profit was maximized at high lean loading by increasing the boiler heat rate. In this region, carbon in natural gas was cheaper than carbon in CO_2. Therefore, natural gas combustion drove profitability of the capture system at these gas prices. When the gas price exceeded $4.6/MMBtu, the C in CO_2 became more valuable than C in natural gas, requiring a reduction in boiler heat rate and consequently, specific heat duty. This indicates that at high gas price, the C in HRSG flue gas drove the profitability. At lower lean loading (0.18 and 0.2 mol/mol), this dynamic was not observed. Heat duty was almost constant at

around 2.2 GJ/tonne for the whole range of gas prices studied. Due to the lower solvent rate at low lean loading, the process operated at a low heat duty irrespective of gas price, corresponding to the region where the C in the HRSG flue gas drove the profitability.

As the ambient temperature increased to 18.3 ˚C, the trend in heat duty at a lean loading of 0.22 lean loading obeyed the dynamic described before, which was optimized to 2.7 GJ/tonne and 2.3 GJ/tonne below and above the breakeven gas price. This was because of the lower CO_2 production at higher ambient temperature, making the process unprofitable at a gas price higher than $3/MMBtu unless the heat duty of the stripper and natural gas boiler was sharply decreased. At this ambient temperature and a lean loading of 0.2 and 0.18 mol/mol, the optimum heat duty remained unaffected as the gas price changed due to the sufficiently high CO_2 production.

In Figure 4, as the ambient temperature increased to 40.5 ˚C, the rich loading and CO_2 flowrate decreased further for all three lean loadings. In this case, at low gas price, a high heat duty was required for both 0.2 and 0.22 lean loading, and only the 0.18 lean loading case was profitable at any gas price without increasing the boiler heat rate. The lean loadings that required an increase in the boiler heat rate showed a much steeper transition to a lower heat duty as the gas price and ambient temperature increased. This can be understood as the effect of decreasing rich loading at

higher ambient temperature. This effect of ambient temperature on rich loading meant that, at a low natural gas price, the process will only remain profitable if the heat duty was increased as a response to a rise in the ambient temperature.

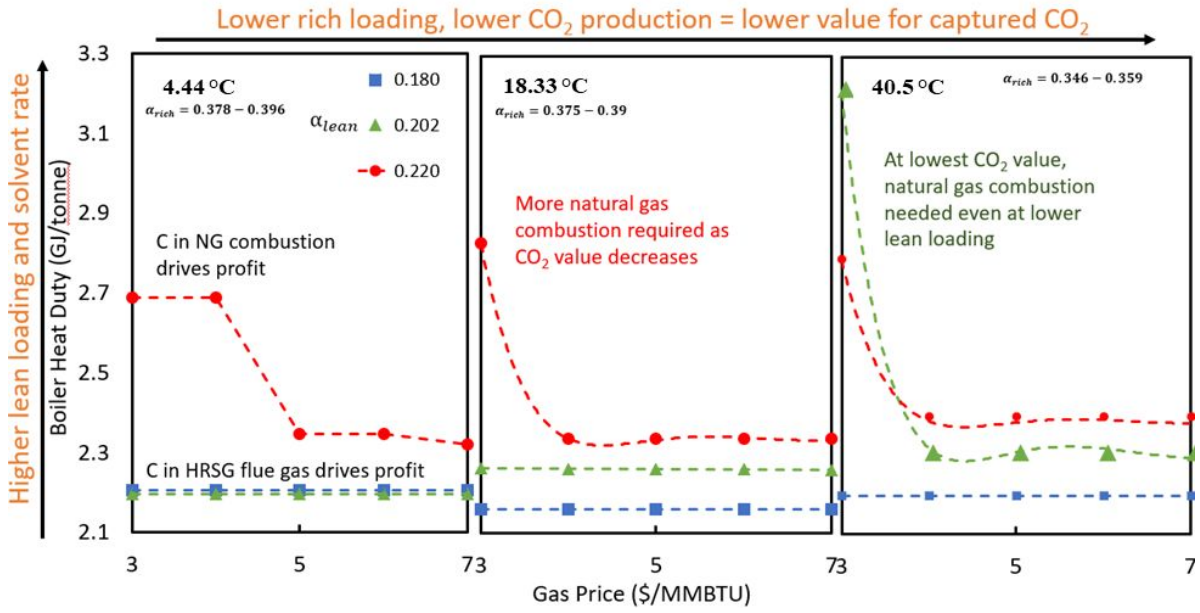

Figure 4. Variation of optimum specific heat duty with gas price as a function of lean loading and ambient temperature, where α_{lean} denotes the lean solvent CO_2 loading.

Process Optimization for Maximization of Variable Profit

The variable profit was highest with 4.4 ˚C ambient temperature, and systematically decreased as the ambient temperature increased, reaching a minimum at 40.5 ˚C. This trend is shown in Figure 5 and resulted primarily through the optimization of lean solvent rate, which showed a similar trend. Variable profit also systematically decreased as the gas price increased to

$5/MMBtu, due to the higher gas price. Optimal process variables however did not change with gas price between $3 and 5/MMBtu.

Lean solvent rate (and CO_2 flowrate) also decreased with ambient temperature to accommodate the lower maximum permissible CO_2 flowrate through the compressor with increasing ambient temperature. Moreover, higher ambient temperature also needed lower pressure stripping, which increased the compressor power requirement. Because the HRSG flue gas flowrate decreased as the ambient temperature increased, so did the optimum lean solvent rate. Additionally, a lower lean solvent rate decreased the electricity consumption from pump work, which was required to maintain optimum profitability at a higher compressor power requirement.

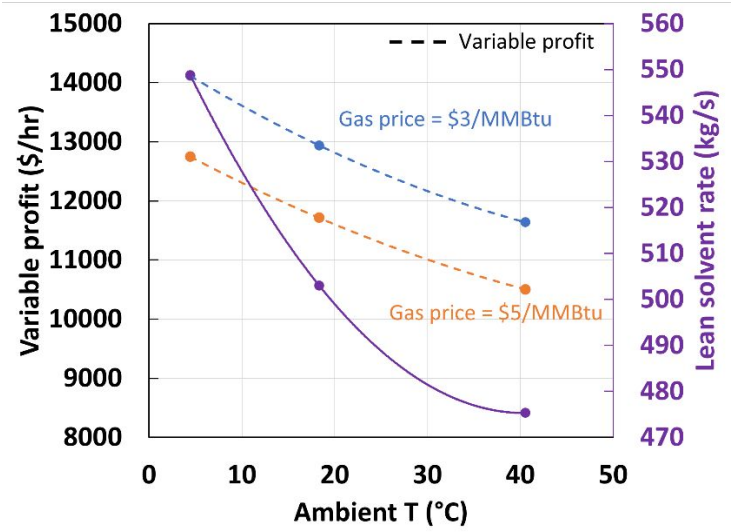

Figure 5. Optimum variable profit for the different scenarios is driven by lean solvent rate, 150 ℃ stripper, CO_2 value: $80/tonne.

The use of a high lean solvent rate at low ambient temperature resulted in the highest amount of CO_2 being captured at that temperature. The amount of CO_2 captured at 4.44 ˚C was the maximum allowed by the working capacity of the compressor. As the ambient temperature increased, the lesser intercooling capacity led to a decreased delta loading, resulting in less CO_2 being captured, lowering the optimal profit. Lean solvent rate was found to be an important driver of profitability and optimal plant operation.

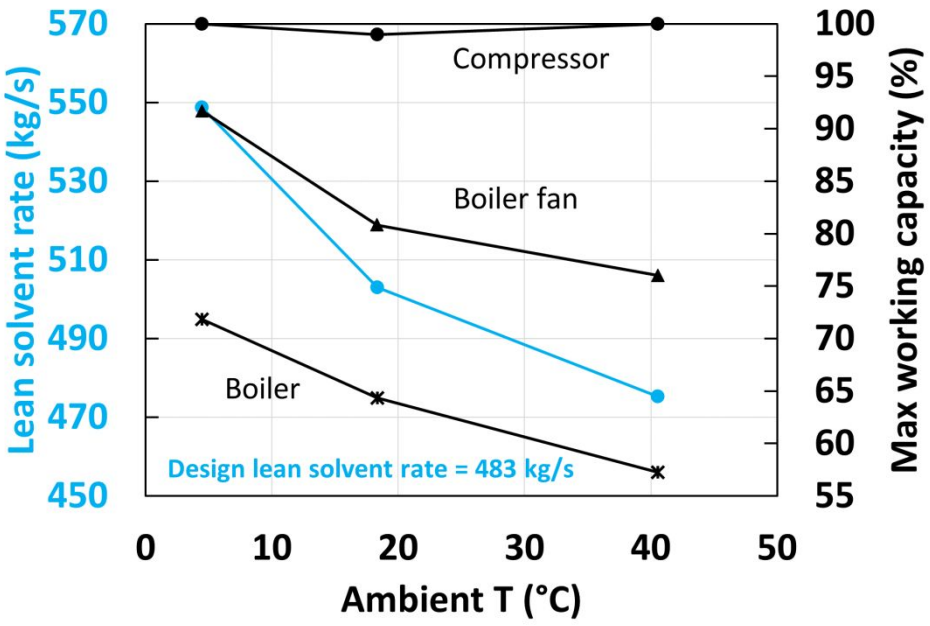

Figure 6. Lean solvent rate drives optimum operation but is limited by compressor operation, 150 ℃ stripper, CO_2 value: $80/tonne, gas price = $3-5/MMBtu.

Figure 6 shows the optimum lean solvent rate for the different scenarios considered. The optimum lean solvent rate for the 4.44 ˚C case was at the upper limit of the range for which the

surrogate model was applicable. However, this case was not limited by the lean solvent rate but by the CO_2 compressor, which was operating at or close to its maximum capacity. While the amount of solvent processed was a significant driver for the profitability of the plant, this was only true while the CO_2 compressor could handle the amount of CO_2 produced. This suggests that a good lean pump design would be one that can match the CO_2 compressor limit. This is especially true considering that both the capital cost and operating cost of the CO_2 compressor are much higher than those of the lean pump. The lean solvent rate exceeded that of the design case (450 kg/s) for all 3 ambient temperatures, which meant that the capacity of the CO_2 compressor was not fully utilized. The boiler fan and boiler were not limiting the optimal operation of the process, as shown by Figure 6.

The variation in CO_2 production with ambient temperature is shown in Figure 7. Figure 7 also shows CO_2 removal as a function of ambient temperature. Notably, the CO_2 removal was always higher than the design removal of 90% and achieved a peak of 96% for the 18.33 ˚C case. This also shows the importance of high CO_2 removal for optimal plant operation and maximization of variable profit.

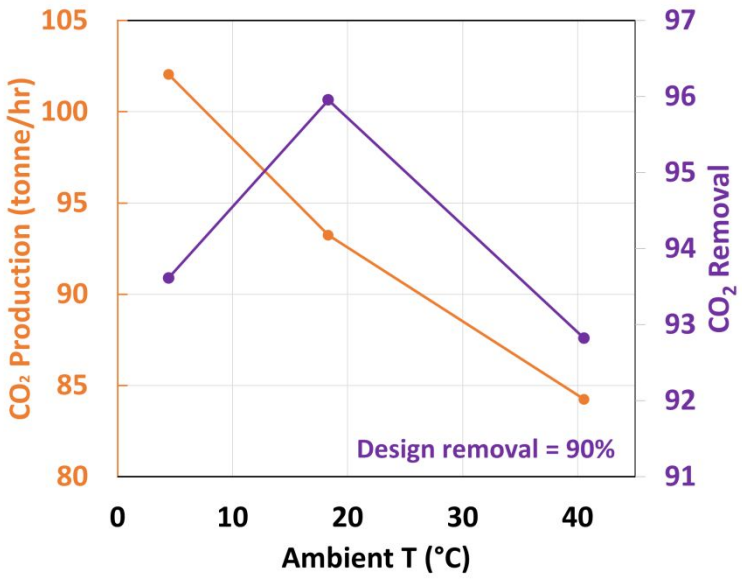

Figure 7. Optimum CO_2 flowrate for a single process train and removal indicate that high removal is important for optimization of operation, 150 ℃ stripper, CO_2 value: \$80/tonne, gas price = \$3–5/MMBtu.

The 18.3 ˚C case had 14% lower flue gas flowrate but only about 9% lower lean solvent rate compared to the 4.4 ˚C case. This, combined with the use of pump-around intercooling and lower pressure stripping (to 0.193 lean loading at 18.3 ˚C versus 0.207 lean loading at 4.4 ˚C) meant the delta loading remained approximately constant between 4.4 and 18.3 ˚C. This resulted in the highest removal for the 18.3 ˚C case. However, the CO_2 flowrate monotonically decreased from 4.4 to 40.5 ˚C, being limited only by the lean solvent rate and maximum working capacity of the compressor, both of which showed a similar behavior with temperature.

Figure 8 shows the CO_2 loading in the rich and lean solvent as a function of ambient temperature along with the number of intercooler air cooler bays used as a function of ambient temperature. Rich loading decreased monotonically with an increase in ambient temperature. At 18.3 and 40.5 ˚C ambient temperature, all the intercooler air cooler bays (20) had to be used to maximize the rich loading, while at lower ambient temperature (4.4 ˚C), effective cooling at the bottom of the absorber was possible with 18 intercooler air cooler bays.

Figure 8 also shows that the lean loading was higher at lower ambient temperature. The optimum lean loading was 0.207 mol/mol at 4.4 ˚C, compared 0.193 mol/mol at 18.3 ˚C and 0.184 mol/mol at 40.5 ˚C. Because of the higher intercooling capacity at 40.5 ˚C, increasing the lean solvent rate to 550 kg/s was sufficient to produce enough CO_2 to match the capacity of the CO_2 compressor, avoiding the need to utilize lower pressure stripping to achieve lower lean loadings. A lower lean loading was necessary at higher ambient temperatures to maximize profitability by increasing the cyclic capacity of the solvent. This was done to make-up for the reduced intercooling capacity at high ambient temperature as shown in Figure 8.

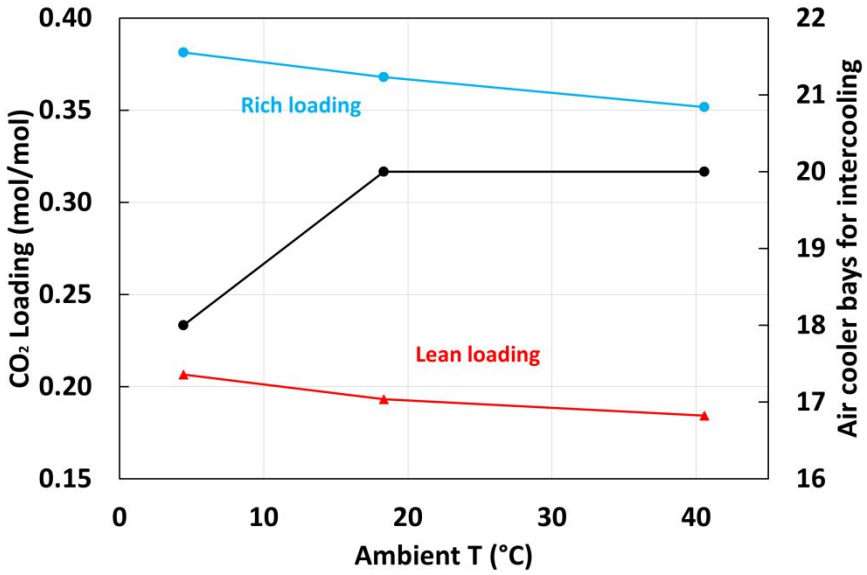

Figure 8. Optimum rich and lean loading for different scenarios; rich loading was maximized at high ambient temperature by using more air cooler bays for intercooling; optimum profit requires low lean loading at high ambient temperature, 150 ℃ stripper, CO_2 value: $80/tonne, gas price = $3-5/MMBtu.

Figure 9 shows the optimum heat duty as a function of gas price and ambient temperature. Overall, the heat duty was between 2.2 and 2.3 GJ/tonne regardless of delta loading, lean solvent rate, or ambient temperature. This was primarily achieved through the optimization of the cold and warm rich bypasses for each case. This enabled efficient recovery of heat from the water vapor leaving the stripper, an important source of irreversibility in the stripper. For all three ambient

temperatures, the optimum bypass split fractions were flat at 27.8 % for the cold rich bypass and 60% for the warm rich bypass (relative to the warm rich solvent flowrate).

In almost every case, over 70% of the rich solvent was bypassed to the top of the stripper column, leaving a maximum of 30% of the total rich solvent leaving the steam heater. Due to the lack of rigorous steam heater modeling in this work, the temperature of the solvent exiting the steam heater could be prohibitive, giving rise to higher rates of thermal degradation and corrosion, especially at the low lean loading that the system self-optimized to in this study. Suresh Babu and Rochelle (2021) conducted a study of the steam heater for the base case FEED for PZAS at a lean loading of 0.2 mol/mol that indicated that the steam temperature required and rich solvent temperature exiting the steam heater are 164 ℃ and 159 ℃ respectively, at 60% warm rich bypass split fraction. These temperatures are expected to be slightly higher in this study due to a lower lean loading and higher total rich bypass.

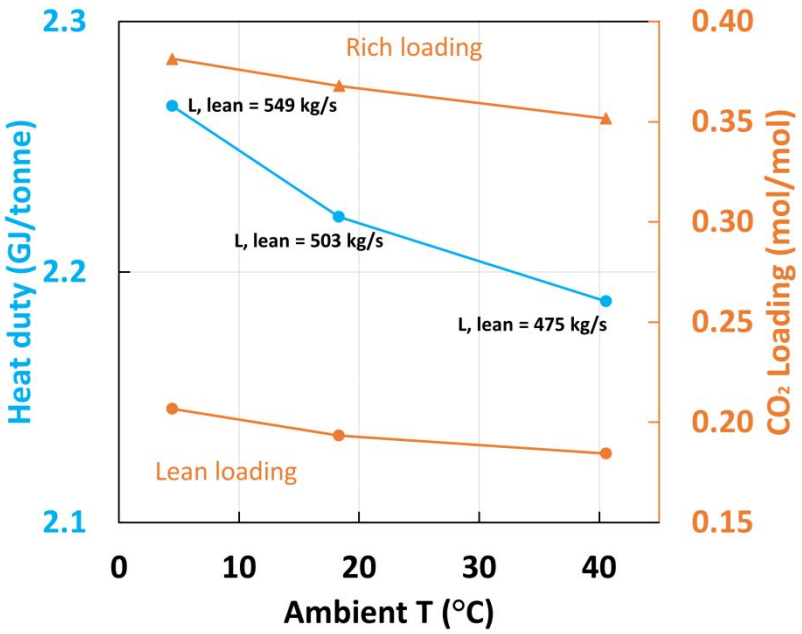

Figure 9. Stripper operated at low heat duty even at high ambient temperature by manipulating lean loading and solvent rate, 150 ℃ stripper, CO_2 value: \$80/tonne, gas price = \$3–5/MMBtu.

As seen in Figure 9, heat duty monotonically decreased with ambient temperature by using a lower lean solvent rate and lower lean loading. Lower lean loading operation has also been related to favorable energy performance of the advanced stripper from pilot plant tests conducted by Suresh Babu and Rochelle [14]. The manipulation of stripper pressure to change lean loading with increasing ambient temperature allowed the cyclic capacity of the solvent to be maintained between 0.167-0.175 mol/mol regardless of the decrease in rich loading with ambient temperature.

This demonstrated that the PZAS process could operate flexibly at different ambient temperatures with a heat duty of 2.2–2.3 GJ/tonne while maximizing variable profit.

Consequently, the boiler heat rate was between 186 and 233 MMBTU/hr. As the ambient temperature increased, so did the lean solvent rate, the delta loading, and the maximum permissible flowrate of the compressor, which decreased the amount of CO_2 captured by the system. The boiler never exceeded 72% of its maximum capacity, as seen in Figure 6.

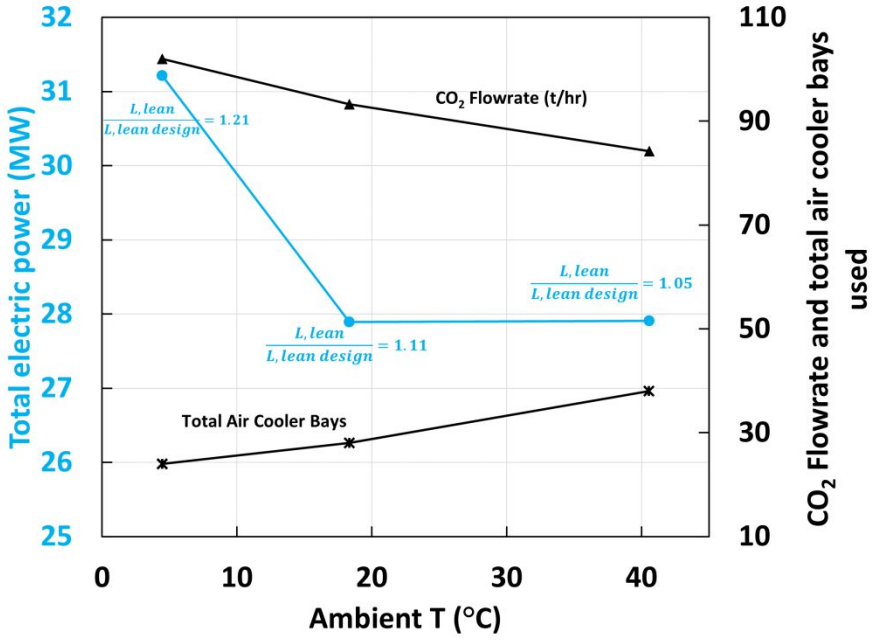

Figure 10. Total electric power requirement was highest at low ambient temperature due to maximization of lean solvent rate and CO_2 flowrate, 150 ℃ stripper, CO_2 value: $80/tonne, gas

price = $3–5/MMBtu, total air cooler bays for intercooling = 20, total air cooler bays for water wash = 18, design lean solvent rate = 450 kg/s.

Figure 10 shows the variation of total electrical power requirement with ambient temperature. Total power appears to be correlated with optimum lean solvent rate and CO_2 flowrate. The total power consumption was highest at 4.44 ˚C and it corresponded to the highest CO_2 flowrate and lean solvent rate of all the cases. The CO_2 flowrate dictated the compressor power requirement, and the lean solvent rate dictated the power requirement from pump work. The compressor power requirement was also related to the working pressure (lean loading) of the stripper.

As the ambient temperature increased, the total power consumption decreased. At 18.33 ˚C, this decrease was due to a lower lean solvent flowrate and a lower CO_2 flowrate, despite the increase in the total air cooler bays used, indicating that the electrical power requirement for pumps and compressors were higher than that of the air coolers. Although the CO_2 flowrate and lean solvent rate were lower at 40.5 ˚C compared to 18.3 ˚C, the power consumption was approximately the same compared to that at 18.3 ˚C due to an increase in air cooler bays and compression requirement from the use low pressure stripping. At 40.5 ˚C, the power requirement of the air coolers and compressor (for low pressure stripping) were more important than that of the pump.

Comments on Solvent Precipitation

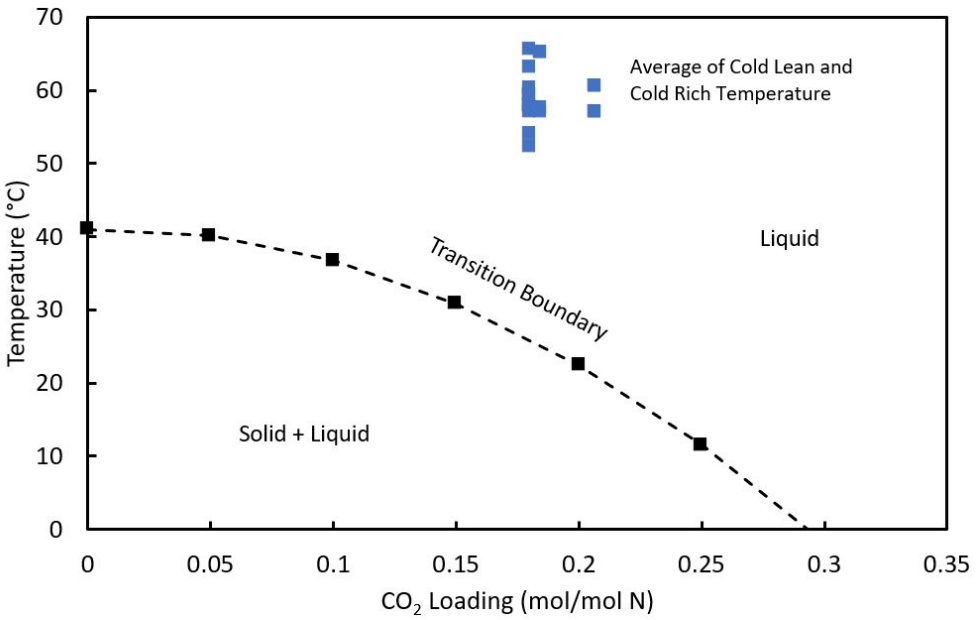

Figure 11. Profitable operation of PZAS at different ambient temperatures while avoiding solvent precipitation was possible.

It was important to consider the possibility of solvent precipitation in the process optimization of PZAS™, especially given that the ambient temperature varied from 4.4 to 40.5 ˚C and lean loading varied from 0.18 to 0.22 mol/mol. From the Solid-Liquid-Equilibrium diagram shown in Figure 11 (adapted from Chen et al. [15]), precipitation in 5 m PZ occurs at low temperature and low lean loading. The coldest point in the system was the metal temperature in the lean end of the cold cross exchanger which was approximated in the model using an average of cold lean and cold rich temperature. Figure 11 plots this average temperature against optimized lean loading for all

the cases considered in this work. A high lean solvent temperature due to the absence of the trim cooler downstream of the cold exchanger avoided precipitation in the system even at a lean loading as low as 0.18 mol/mol.

Nevertheless, it is still possible that operation at lower lean loading will expose the system to precipitation in the event of an unplanned shutdown during low ambient temperature. At the selected limit of 0.18 lean loading, the solution will precipitate if it cools to 26 ^{o}C.

Comments on Amine Volatility

The lean solvent temperature at the absorber inlet at the optimized operating conditions was between 61 and 78 ˚C. While this avoided solvent precipitation, it also made for hot lean solvent entering the absorber. This high temperature will result in a larger concentration of vapor PZ in the flue gas entering the water wash. A modified water wash design may be necessary to avoid excessive emissions of PZ in the cleaned flue gas.

Interactions between CAPEX and OPEX

This section combines the variable annual profit with other fixed annual costs to provide an approximate overall cash flow analysis. For the calculations below, when the NGCC was operating, it was assumed to be at full load, with 95% of the HSRG flue gas being fed to the

absorber. An average ambient temperature of 15.5 ℃ (60 °F) was used for the year 2019. An average annual load factor of 56% was used, obtained from actual flue gas availability data of the NGCC. The gas price, power price, and CO_2 value were assumed to be \$3/MMBtu, \$26/MWh, and \$80/tonne, respectively. Using the relationship between the optimized hourly profit as a function of ambient temperature (Figure 5), the optimum profit was calculated to be \$64.5 MM/year.

This value only included the revenue from CO_2, and cash flow from natural gas and electricity. Using the data provided by Rochelle et al. (2022), the variable annual expenses for chemicals (PZ and others) were adjusted for the increase in capacity factor (56% compared to 52%) and included in this analysis to give an incremental cash flow with variable annual costs of \$60.3 MM. The fixed annual costs taken from Rochelle et al. (2022) were also adjusted for the increase in capacity factor and accounted for in the cash flow analysis. This resulted in a net annual cash flow (fixed and variable) of \$25.2 MM for the case with the optimized operation, 45% higher than the design value of \$17.4 MM estimated by Rochelle et al. (2022). With total investment of about \$725 MM (Rochelle et al., 2022), this yielded a pay-back period of 29 years.

A breakdown of the cash flow analysis is shown in Table 5.

Table 5: Cash flow analysis with optimized operation

Cost Item	Cost
Total investment ($MM)	**725**
Variable Annual Costs ($MM/yr)	
Variable profit (includes CO_2 revenue, gas, and electricity)	64.5
PZ solvent	(-) 2.16
Other chemicals	(-) 2.05
Annual cash flow with variable costs	**(+) 60.3**
Fixed Annual Costs ($MM/yr)	
Property taxes and insurance	(-) 19.6
Maintenance, labor and material	(-) 10.7
Operating cost, labor	(-) 3.6

Administration and support, labor	(-) 1.3
Total fixed annual costs	**(-) 35.1**
Net annual cash flow	**(+) 25.2**
Payout period (yr)	**29**

A higher net annual cash flow would result in a lower pay-back period. This can be achieved by reducing the contributions of gas and electricity in the variable annual cash flow. This work can be used to guide the design of an improved process configuration that can reduce these costs. Some potential options are given below.

The number of heat exchangers in the process can be increased, which will directly result in a lower heat duty, cash flow from gas consumption, heat exchange area for steam heaters, and boilers in a newer design. This is also expected to reduce the capital of the air coolers for water wash, which ultimately acts as the heat sink for the cold lean solvent.

Using cooling water instead of air cooling would significantly reduce the capital and operating expenses of the capture plant since it is less expensive to transport, and service compared to

ambient air. Cooling water would also make the capture plant less exposed to changes in ambient temperature, which would increase CO_2 production, especially in the summer months.

The compressor capacity can be increased to increase the CO_2 production in a given year. This work showed that the compressor limited the profitability of the capture train. While this change would increase the compressor cost, it would be of special relevance given the relatively low capacity factors of the NGCC.

Conclusions

Rigorous rating models for the PZAS process were constructed using surrogate models created for economic optimization. Optimization of variable profit for retrofit on a 460 MW NGCC operation indicated that:

- Low lean loading of about 0.18 mol CO_2/equiv. N generally resulted in lower reboiler heat duty. Optimum heat duty was found to be 2.2-2.3 GJ/tonne.

- Solvent precipitation was avoided even at low lean loading (0.18 mol/mol) in the absence of a trim cooler for the lean solvent between the absorber and the cold cross exchanger.

- Optimal CO_2 removal was always higher than the design case removal of 90% indicating that the plant was overdesigned. From 4.4 to 18.3 ˚C, the removal increased to its maximum of

96% from 94% due to a much larger decrease in flue gas flowrate (14%) than lean solvent rate (9%). Intercooling and low pressure stripping also helped maintain the cyclic capacity of the solvent to be constant at 0.175 mol/mol between 4.4 and 18.3 ˚C.

- Lean solvent rate was higher than the design value of 450 kg/s in all cases, making it a key driver of plant profitability. Optimum lean solvent rate was 5-21% higher than the design value.

- Increasing compressor, boiler, and boiler fan capacities could increase variable profit by about 21% for 0.18 lean loading at 4.4 ˚C ambient temperature. This increase in profit is reduced (6-11%) at higher ambient temperature and lean loading.

- The breakeven gas price was $4.6/MMBtu, and below this value, the variable profit was maximized at high lean loading by increasing the boiler heat rate, as the carbon in natural gas was cheaper than the carbon in the captured CO_2. Above a gas price of $4.6/MMBtu, carbon in captured CO_2 became cheaper than carbon in natural gas, requiring a reduction in boiler heat rate and consequently, specific heat duty, especially at 0.22 lean loading. This dynamic was less predominant at lower lean loading (0.2, 0.18 mol/mol), since the CO_2 captured from the HRSG flue gas was enough to use all the CO_2 compressor capacity and maximize profit.

AUTHOR INFORMATION

Corresponding Author

*Dr. Gary T. Rochelle, email: gtr@che.utexas.edu

Present Addresses

†Texas Carbon Management Program, McKetta Department of Chemical Engineering, The University of Texas at Austin, 10500 Exploration Way, Austin, TX 78758, USA

Author Contributions

The manuscript was written through contributions of all authors. All authors have given approval to the final version of the manuscript.

Supporting Information

Supporting information for the material in this paper is provided in the form of appendices. This consists of 5 sections. Appendix A describes the different rating models that were developed for the absorber, air coolers, stripper, and compressor. Appendix B describes the development of surrogate models for the same equipment items. Appendix C details the workings of the MATLAB scripts used for steady state convergence. This includes a description of the operational constraints implemented in the model. Appendix D provides the nomenclature for all short-form variables that appear in the equations in this work. Appendix E provides a list of all surrogate models developed

in this work for the different equipment items and their tabulated R^2 values. Appendix F provides the MATLAB script used for steady state convergence and optimization of variable profit.

ACKNOWLEDGMENT

This work was supported by Department of Energy (DOE) Award No. DE-FE0031844 and by additional funding from ExxonMobil, Total, Chevron, Honeywell UOP, and the Texas Carbon Management Program. This report was prepared as an account of work sponsored by an agency of the United States Government. Neither the United States Government nor any agency thereof, nor any of their employees, makes any warranty, express or implied, or assumes any legal liability or responsibility for the accuracy, completeness, or usefulness of any information, apparatus, product, or process disclosed, or represents that its use would not infringe privately owned rights. Reference herein to any specific commercial product, process, or service by trade name, trademark, manufacturer, or otherwise does not necessarily constitute or imply its endorsement, recommendation, or favoring by the United States Government or any agency thereof. The views and opinions of authors expressed herein do not necessarily state or reflect those of the United States Government or any agency thereof.

This work was also supported by CCSI²/NETL/DOE through LEIDOS PO10227981.

One author of this publication consults for a process supplier on the development of amine scrubbing technology. The terms of this arrangement have been reviewed and approved by the University of Texas at Austin in accordance with its policy on objectivity in research. The authors have financial interests in intellectual property owned by the University of Texas that includes ideas reported in this paper.

Aspen Plus® proprietary software was provided by an academic license from AspenTech®. AspenTech® and Aspen Plus® are trademarks of Aspen Technology, Inc. All rights reserved.

REFERENCES

[1] Gao, T.; Rochelle, G.T. Creative absorber design and optimization for CO_2 capture with aqueous piperazine. *International Journal of Greenhouse Gas Control.* 2022, 113, 103534.

[2] Suresh Babu, A.; Rochelle, G.T. Process design of the piperazine advanced stripper for a 460 MW NGCC. *International Journal of Greenhouse Gas Control.* 2022, 115, 103631.

[3] Closmann, F.; Rochelle, G.; Gao, T.; Suresh Babu, A.; Abreu, M.; and Drewry, B. FEED for Piperazine with the Advanced Stripperr™ on NGCC at Denver City, Texas. *Proceedings of the 15th Greenhouse Gas Control Technologies Conference*. 2021.

[4] Rochelle, G.T.; Closmann, F.; Suresh Babu, A.; Drewry, B.; Gao, T.; Martorell, J.; Abreu, M.; Steen, W.A.; Farmer, K.; Bryan, S.; Bernau, M.; Sexton, A.; Dombrowski, K.; Myers, D.; Marsh, M.; Piggott, B.; Jones, R.; and Lee, J. Front-End Engineering Design for Piperazine with the Advanced Stripper. *Final report for DE-FE0031844*. 2022.

[5] Rochelle, G.; Closmann, F.; Abreu, M.; Suresh Babu, A.; Drewry, B.; Gao, T.; Steen, W.A.; Farmer, K.; Bryan, S.R.; Bernau, M.; Sexton, A.; Dombrowski, K.; Jones, R.; Marsh, M.; Piggott, B.; and Myers, D. Cost details from Front-End Engineering Design of piperazine with the advanced stripper. *Proceedings of the 16th Greenhouse Gas Control Technologies Conference (GHGT-16)*. 2022.

[6] Aspen Plus® 12.1 User guide, Aspen Technology, Inc., Cambridge, MA. 2003.

[7] Cozad, A.; Sahinidis, N.V.; Miller, D.C. Automatic Learning of Algebraic Models for Optimization. *AIChE Journal*. 2014, 60, 2211.

[8] MATLAB version 9.11.0 (R2021b). Natick, Massachusetts: The MathWorks, Inc. 2010.

[9] Frailie, P.T. Modeling of carbon dioxide absorption/stripping by aqueous methyldiethanolamine/piperazine. Ph.D. Dissertation. The University of Texas at Austin. 2014.

[10] Song, D. Effect of liquid viscosity on liquid film mass transfer for packings. Ph.D. Dissertation. The University of Texas at Austin. 2017.

[11] Taylor, R.; Krishna, R. *Multicomponent Mass Transfer*. New York. 1993.

[12] Aspen Exchanger Design & Rating (EDR), Aspen Technology, Inc., Cambridge, MA. 2013.

[13] Lin, Y.J. Modeling advanced flash stripper for carbon dioxide capture using aqueous amines. Ph.D. Dissertation. The University of Texas at Austin. 2016.

[14] Suresh Babu, A. and Rochelle, G. Heat Loss Characteristics and Energy Use of Piperazine with the Advanced Stripper (PZAS) at the UT-SRP Pilot Plant. *Proceedings of the 16th Greenhouse Gas Control Technologies Conference (GHGT-16)*. 2022.

[15] Chen, E. ; Fulk, S. ; Sache, D. ; Lin, Y.J.; Rochelle, G.T. Pilot plant activities with concentrated piperazine. *Energy Procedia*. 2014, 63, 1376.

FOR TABLE OF CONTENTS ONLY